ISBN: 978-3-95450-223-3 ISSN: 2673-7000 doi:10.18429/JACoW-NAPAC2019-TUPLH20

COMMISSIONING OF THE CESR UPGRADE FOR CHESS-U

J. Shanks*, G. Codner, M. Forster, D.L. Rubin, S. Wang, L. Ying
CLASSE, Cornell University, Ithaca NY, USA

Abstract

The Cornell Electron Storage Ring (CESR) was upgraded in the second half of 2018 as a dedicated synchrotron light source, CHESS-U. The upgrade is by far the largest modification to CESR in its 40-year history, replacing one-sixth of the storage ring with six new double-bend achromats, increasing beam energy from 5.3 GeV to 6.0 GeV, and switching from two counter-rotating beams to a single on-axis positron beam. The new achromats include combined-function dipoles, a first in CESR, and reduce the horizontal emittance at 6.0 GeV by a factor of four. Eight compact narrow-gap undulators (4.6mm vacuum chamber aperture) and one high-energy 24-pole wiggler feed a total of six new and five existing x-ray end stations from a single positron beam. Commissioning of CHESS-U took place in the first half of 2019. We report on the results of beam commissioning, including optics correction and characterization.

CHESS-U OVERVIEW

The accelerator design for the CHESS-U upgrade is documented elsewhere [1]. Parameters before and after the CHESS-U upgrade are summarized in Table 1.

Table 1: Design Lattice Parameters for CESR Before and After CHESS-U Upgrade

Parameter	CHESS	CHESS-U
Circumference [m]	768.438	768.438
Energy [GeV]	5.289	6.0
Species	e^+ and e^-	e^+
Current [mA]	120/120	200
ϵ_x [nm·rad]	98	29.6
Emittance coupling	1%	1%
$\beta_{x,y}$ at IDs [m]	7.9, 3.1	11.2, 2.6
η_x at IDs [m]	0.42	0
IDs	3	9
End Stations	11	11
$Q_{x,y}$	11.28, 8.78	16.55, 12.63
$Q'_{x,y}$	−16.0, −14.2	−25.6, −26.8
α_p	9.2×10^{-3}	5.7×10^{-3}
σ_z [mm]	16	17
I_{bunch} [mA]	7	2.2
τ_{Touschek} [hrs]	>24	40
V_{RF} [MV]	5.2	6.0

Four of the seven straights (Sectors 2, 3, 4, and 7) house a pair of CHESS Compact Undulators [2, 3], split by a 2 mrad canting angle (1 mrad in Sector 7). Sector 1 uses an existing 24-pole wiggler [4]. The geometry of the remaining two sectors is not conducive to end stations at this time. Removal of the old sextant of CESR and installation of the six new achromats was completed from June 2018 to January 2019.

Table 2: Commissioning Timeline

Date	Milestone
1/30/19	CESR gun, linac, and synchrotron on
2/22/19	First attempt at e^- injection
3/6/19	First turn achieved – e^- at 5.289 GeV
3/11/19	Recover e^- accumulation at 5.289 GeV Time in CBPM system and correct optics.
4/8/19	Recover e^+ accumulation. Store 50 mA e^+ at 5.289 GeV.
4/24/19	First turn achieved – e^+ at 6.0 GeV
4/26/19	Recover e^+ accumulation at 6.0 GeV
4/27/19	Establish 100 mA e^+ conditions at 6.0 GeV
5/9/19	Sector 1 wiggler gap closed First canted IDs installed in Sector 7
5/16/19	First light in Sector 7
5/17/19	First light in Sector 1
6/27/19	All five front-ends illuminated

The digital CESR Beam Position Monitor (CBPM) system requires timing in to the peak of a bunch passage to around 10 ps. Details on the CBPM system are available in [5]. Timings for the new sextant of the ring were initially unknown, therefore the first turns in the storage ring were observed using an older analog BPM system with diode stretcher and higher sensitivity. Roughly every tenth set of buttons in CESR is permanently connected to the relay system, though it is possible to "steal" buttons from the CBPM system for use in the relay system. For threading the first turn, relay BPMs in the new sextant were set up in a "cow" configuration, where all four button signals are summed to provide a dead-or-alive intensity signal. Once beam was stored, the digital bunch-by-bunch system was restored.

COMMISSIONING

The CHESS-U commissioning timeline is summarized in Table 2. Positron operation is in the clockwise direction, compatible with CHESS operation. Electron operation is in the counter-clockwise direction, which although incompatible with the polarity of x-ray beam lines, allows for approximately 10 times higher charge per injection pulse, improving BPM signal amplitude prior to accumulation.

* js583@cornell.edu

ISBN: 978-3-95450-223-3 ISSN: 2673-7000 doi:10.18429/JACoW-NAPAC2019-TUPLH20

Due to its size, the Sector 1 wiggler was installed prior to initial commissioning, with its gap maximally opened until the Sector 1 front end was ready to receive x-rays. Canted pairs of 1.5-m-long CCUs were installed every two weeks, taking 3-4 days per pair for the initial installation. The impact on optics and operations from each pair of IDs was minimal, with first light on each front end coming within 48 hours of turning on after installation.

CHARACTERIZATION

Optics

The betatron phase advance is measured using resonant excitation at the betatron tunes and recording trajectory data with the turn-by-turn-capable BPM electronics [6, 7]. Corrections to the linear optics are determined from betatron phase and horizontal dispersion measurements. Phase and dispersion after correction are shown in Fig. 1. Transverse coupling, as characterized by the $\bar{C}$ formalism [8], is also measured with phase data and corrected to around 2%, sufficient for initial commissioning.

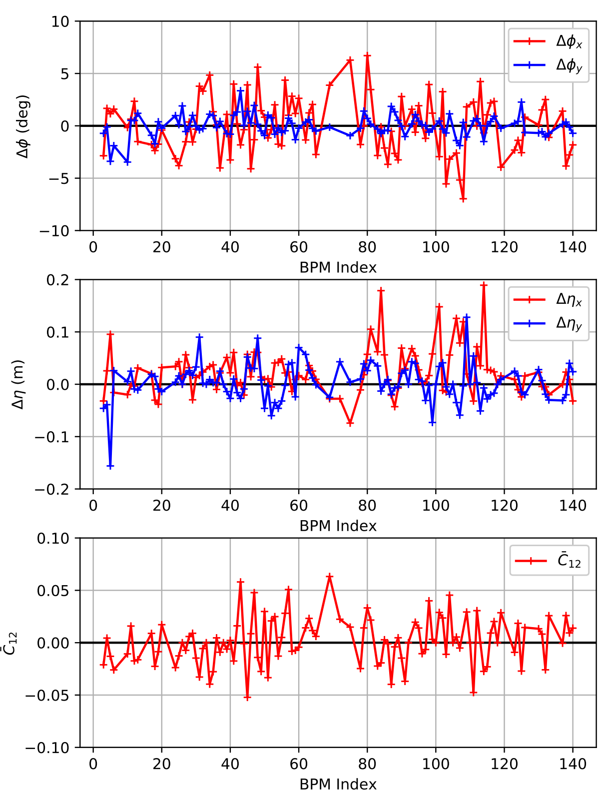

Figure 1: Errors in betatron phase advance, dispersion, and $\bar{C}_{12}$, measured after correction. The new section of the accelerator straddles index 0, spanning indices 0-24 and 119-140.

Tune Plane

Resonances in the tune plane were mapped based beam lifetime. The measured tune plane after installing all 8 CCUs and one 24-pole wiggler is shown in Fig. 2, and is in good agreement with simulation results.

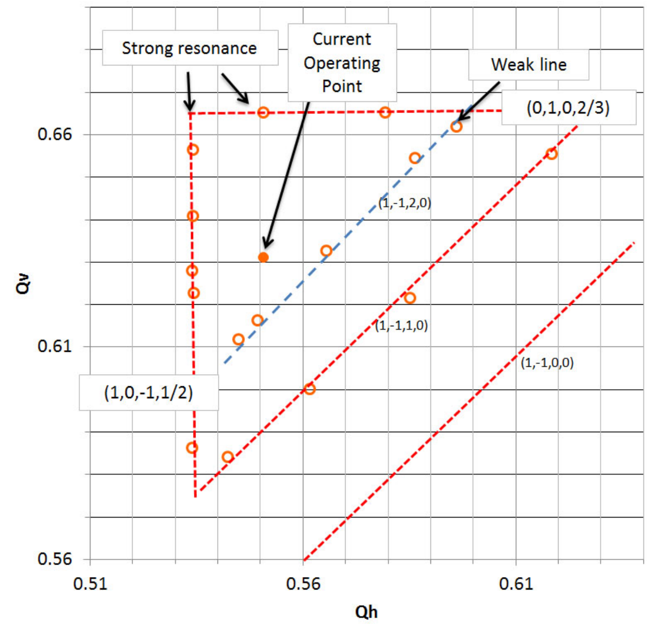

Figure 2: Tune scan around design working point. Data points represent tunes where lifetime was observed to be poor when the pulsed injection bumpers were firing.

Beam Lifetime

Beam lifetime was measured as a function of total beam current, before and after activation of NEG strips through the new section of the storage ring. See Fig. 3. Two bunch patterns were examined: nine trains of five 14-ns-spaced bunches each, and nine trains of one bunch each.

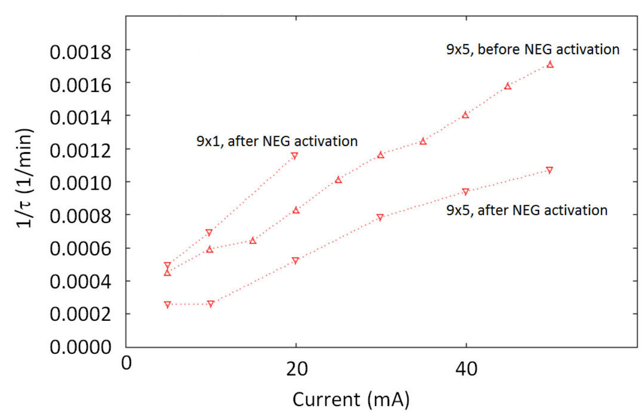

Figure 3: Lifetime as a function of total beam current, before and after activation of NEG strips in the new achromat cells. Bunch patterns are indicated as (number of trains)x(number of bunches per train).

Transverse Impedance

The real and imaginary components of the transverse impedance were characterized through tuneshift and damping as a function of bunch current. Results are summarized in Table 3. For all transverse impedance measurements, chro-

ISBN: 978-3-95450-223-3 ISSN: 2673-7000 doi:10.18429/JACoW-NAPAC2019-TUPLH20

maticity was set to $\xi_{x,y}$ = (+1,+1) and all feedback systems were disabled.

Table 3: Transverse and Longitudinal Impedance Measurements, Before and After the CHESS-U Upgrade

	2018	**2019**	**Units**
df_h/dI, measured	−30	−7	Hz/mA
df_v/dI, measured	−273	−358	Hz/mA
df_v/dI, analytic	−292	−321	Hz/mA
$d\alpha_h/dI$, measured	−600	−1721	$\sec^{-1}$/mA
$d\alpha_v/dI$, measured	−3040	−853	$\sec^{-1}$/mA
k_{HOM}, measured	−4.83	−4.76	V/pC
k_{HOM}, analytic	−2.60	−2.01	V/pC

The resistive wall impedance impedance is dominated by the four 3.5-m-long narrow-gap (4.6 mm full-aperture) undulator chambers. Measured transverse impedances are in agreement with analytic calculations.

HOM Loss Factor

The method used for determining the higher-order mode (HOM) loss factor, k_{HOM}, was originally developed at PETRA [9]. To summarize: Three consecutive RF buckets (separated by 2 ns) are filled. The first bunch is a "precursor," providing a reference time. The second is the "main" bunch, whose current is varied. The third bunch acts as a "witness" to the wake left by the main bunch. The arrival time of all three bunches is observed on a sampling scope as a function of current in the main bunch. An example measurement at one main bunch current is shown in Fig. 4. The variation in arrival time as a function of main bunch current is shown in Fig. 5.

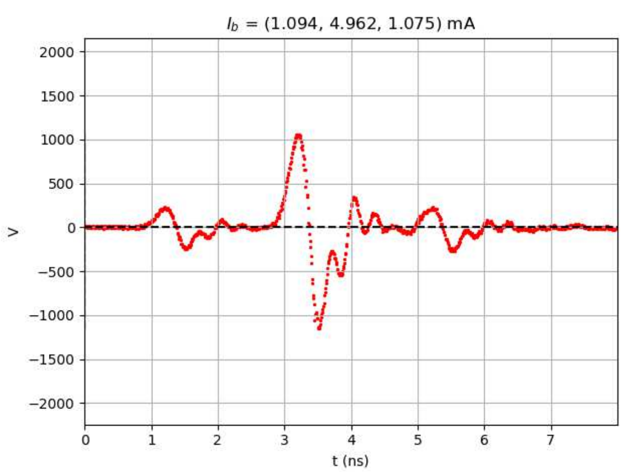

Figure 4: Example data from bunch sampling scope, with three consecutive bunches (precursor, main, and witness), separated by one RF bucket = 2 ns.

The changes in arrival times between the precursor, main, and witness bunches determine the HOM loss factor and are a measurement of the longitudinal wake as seen by the

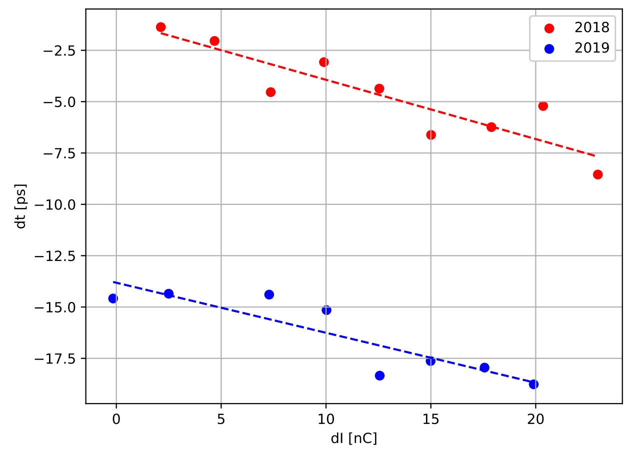

Figure 5: HOM characterization in 2018 (prior to CHESS-U upgrade) and 2019 (during commissioning). Shown is the change in relative arrival time for the main bunch with respect to the precursor bunch, which determines k_{HOM}.

witness bunch 2 ns after the main bunch. Details of the calculation are available in [10].

Results are summarized in Table 3, along with analytic estimates for k_{HOM}. The discrepancy between measured and calculated loss factors is not understood at this time, however the discrepancy predates the CHESS-U modifications and has caused no observable impact on operations. Insufficient data was collected during the 2019 commissioning period to compute $W_{||}$ after the CHESS-U upgrade; this measurement will be revisited during the Fall 2019 startup.

PRESENT STATUS

CESR beam commissioning began in February 2019. As of the writing of this paper, CESR has stored >100 mA e^+ at 6.0 GeV, all eight canted undulators and one permanent-magnet wiggler are installed, and beam has been observed in the front-end of all end stations. Preliminary characterization during commissioning already shows a 9-fold increase in flux-per-mA over the best pre-CHESS-U conditions at 10 keV.

ACKNOWLEDGEMENTS

The authors wish to thank everyone involved in the design, construction, installation, and commissioning of the CESR upgrade. The operations group is indebted to Mike Billing, whose knowledge, expertise, patience, and passion will be deeply missed.

Funding for the CHESS-U upgrade was provided by New York State Capital Grant #AA737 / CFA #53676. CHESS is funded by NSF award DMR-1332208, the CHEXS subfacility is funded by NSF award DMR-1829070, and MacCHESS is funded by NIGMS award GM-103485.

ISBN: 978-3-95450-223-3 ISSN: 2673-7000 doi:10.18429/JACoW-NAPAC2019-TUPLH20

REFERENCES

[1] J. Shanks, J. Barley, S. Barrett, M. Billing, G. Codner, Y. Li, X. Liu, A. Lyndaker, D. Rice, N. Rider, D. L. Rubin, A. Temnykh, and S. Wang, "Accelerator design for the Cornell High Energy Synchrotron Source upgrade," *Phys. Rev. Accel. Beams*, vol. 22, p. 021602, Feb 2019.

[2] A. Temnykh, T. Kobela, A. Lyndaker, J. Savino, E. Suttner, and Y. Li, "Compact undulator for Cornell High Energy Synchrotron Source," *IEEE Trans. App. Superconductivity*, vol. 22, p. 4100504, June 2012.

[3] A. Temnykh, D. Dale, E. Fontes, Y. Li, A. Lyndaker, P. Revesz, D. Rice, and A. Woll, "Compact undulator for the Cornell High Energy Synchrotron Source: Design and beam test results," in *J. Phys.: Conf. Ser.,* vol. 425, p. 032004, 2013.

[4] K. Finkelstein, "The new CHESS wiggler," *Rev. Sci. Instrum.,* vol. 63, pp. 305–308, 1992.

[5] M. Billing, W. Bergan, M. Forster, R. Meller, M. Rendina, N. Rider, D. Sagan, J. Shanks, J. Sikora, M. Stedinger, C. Strohman, M. Palmer, and R. Holtzapple, "Beam position monitoring system at CESR," *J. Instrum.*, vol. 12, p. T09005, Sept. 2017, doi:10.1103/Phys

[6] D. Sagan, R. Meller, R. Littauer, and D. Rubin, "Betatron phase and coupling measurements at the Cornell Electron/positron Storage Ring," *Phys. Rev. ST Accel. Beams*, vol. 3, Sept. 2000. doi:10.1103/PhysRevSTAB.3.092801

[7] J. Shanks, D. L. Rubin, and D. Sagan, "Low-emittance tuning at the Cornell Electron Storage Ring Test Accelerator," *Phys. Rev. ST Accel. Beams*, vol. 17, Apr. 2014. doi:10.1103/PhysRevSTAB.17.044003

[8] D. Sagan and D. Rubin, "Linear analysis of coupled lattices," *Phys. Rev. ST Accel. Beams*, vol. 2, July 1999. doi:10.1103/PhysRevSTAB.2.074001

[9] R. D. Kohaupt, "Single beam instabilities in PETRA," *IEEE Transactions on Nuclear Science*, vol. 26, no. 3, pp. 3480–3481, 1979.

[10] M. Billing, "Measuring higher order mode loss factors and wake voltages using the change in phase of two bunches," CBN 01-6, CLASSE, Cornell University, Ithaca, NY, 2001.